PROCEEDINGS OF SCIENCE

The ExtraGalactic Cosmic-Ray Propagator (EGCRProp)

M. A. Leigui de Oliveira* **and R. P. Costa Jr.**
Center for Natural Sciences and Humanities (CCNH)
Federal University of ABC (UFABC)
09210-580 Santo André, São Paulo, Brazil.
E-mail: leigui@ufabc.edu.br

We present the ExtraGalactic Cosmic-Ray Propagator (**EGCRProp**), a fast Monte Carlo code for the propagation of ultra-high energy cosmic rays in the extragalactic medium. The full three-dimensional trajectories of charged nuclei (from protons up to iron) across regions of coherent magnetic fields are calculated up to ultrarelativistic energies. Interactions with the extragalactic background light leading to energy losses can be taken into account. The dynamical evolution of several parameters, like the particle energy, magnetic rigidity, deviation angle, or total distance traveled were obtained and studied. Different methods for integrating the equations of motion can be applied in the simulation, with arbitrary floating-point precision computation. In this work, we present the **EGCRProp** main features and results.
Key words: Extragalactic Magnetic Fields, Ultra-High Energy Cosmic Rays, Astroparticles.

36th International Cosmic Ray Conference -ICRC2019-
July 24th - August 1st, 2019
Madison, WI, U.S.A.

*Speaker.

PoS(ICRC2019)330

1. Introduction

The origin of ultra-high energy cosmic rays (UHECRs) is among the most challenging problems in modern astrophysics. To obtain more informations about the most powerful cosmic sources in the universe we need to calculate the propagation of the particles they emit through intergalactic space, and, in the presence of the extragalactic magnetic fields (EGMFs), their arrival directions are expected to be modified. The UHECRs also interact with low-energy photons and matter such that their energy spectrum and chemical composition change after the propagation.

ExtraGalactic Cosmic-Ray Propagator (**EGCRProp**) [1] is a numerical simulation code for tracking UHECRs through EGMFs. It generates the spatial coordinates of particles of given charge, mass, and energy traveling across a cosmic magnetized medium, described in section 2. Furthermore, it is also provided the particles' energy, traveled distance, and deflection angle, at each time step, which are recorded to be further analyzed. **EGCRProp** is structured in two object-oriented C++ codes: a tensorial magnetic field generator, and the propagator itself. Together, it is also provided a three-dimensional viewer to plot the particles' trajectories (see figure 1). All the packages are available to be downloaded on [2].

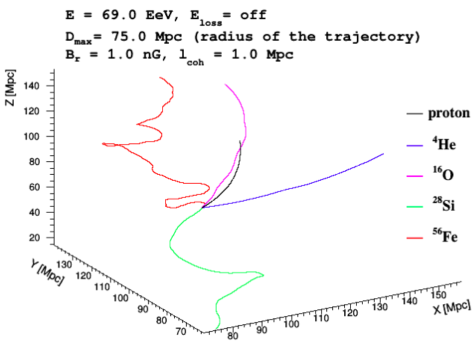

Figure 1: Trajectories, provided by **EGCRProp**, of particles of energy 69 EeV with different compositions (colors) across EGMFs. The fields are arranged within spherical cells of coherence length 1.0 Mpc and intensity 1.0 nG. In this plot, the trajectories were followed up to a radius of 75.0 Mpc, and no energy loss has been considered.

2. The model for the extragalactic magnetic fields

The simulation universe is modeled as a cube of volume $(170\, l_{coh})^3$, where l_{coh} is the coherence length for the magnetic field (by default, $l_{coh} = 1$ Mpc). The magnetic domains are defined as spherical cells of coherent fields. The center of each cell is placed in a lattice of cubic structure and lattice parameter l_{coh}. The magnetic field orientation is then sorted for each cell, while its intensity is kept constant in 1.0 nG throughout the space. Up to 0.95 Mpc from the center of each cell, the magnetic field is coherent, but outside this region, we considered smooth transitions for $\vec{B}(\theta, \phi)$, such that the values for the orientation angles (zenith or azimuth) are given by weighted averages:

$$\alpha = \left(\frac{\alpha_1}{d_1} + \frac{\alpha_2}{d_2} \right) \left(\frac{1}{d_1} + \frac{1}{d_2} \right)^{-1}, \tag{2.1}$$

where the weights are inversely proportional to the distances of the two nearest cells (see figure 2).

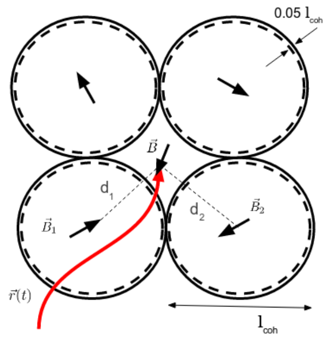

Figure 2: Smooth transitions between the magnetic domains. In red, is displayed the particle's trajectory. Inside 0.95 Mpc (i.e., within the dashed lines), the magnetic field is coherent, and beyond this limit, the field orientation angles are calculated through equation 2.1.

3. The equations of motion

The relativistic Lorentz force describes the equation of motion for a particle of mass m and charge q propagating across electromagnetic fields:

$$\frac{d\vec{p}}{dt} = q(\vec{E} + \vec{v} \times \vec{B}), \tag{3.1}$$

where $\vec{p} = \gamma m \vec{v}$ is the relativistic momentum, with γ the Lorentz factor, $\vec{v}$ is the instantaneous velocity, $\vec{E}$ is the electric field, and $\vec{B}$ is the magnetic field. If the particle is also subjected to electric forces, then its energy changes follow the time rate given by $q(\vec{v} \cdot \vec{E})$. In our case, the electric fields are considered to be absent or negligibly small.

We integrate numerically the particle's equation of motion, such that, at each time step δt, the final particle's velocity is given by:

$$\vec{v}_f = \vec{v}_0 + \int_0^{\delta t} (\vec{v} \times \vec{\omega}_B) dt, \tag{3.2}$$

where $\vec{\omega}_B = q\vec{B}/\gamma m$ is the cyclotron frequency and the time step is chosen to be a small fraction ($\delta t/T \lesssim 10^{-3}$) of the instantaneous period of revolution $T = 2\pi/\omega_B$. We have studied the accuracy and the computational performance of four numerical integration methods for the case of an uniform magnetic field. The results of this study have been published in [3].

4. Energy losses

Even though in our case the particles do not lose (or gain) energy directly through interactions with electric fields, at each time step, energy losses can be plugged in the simulation. Especially for great distances of propagation, it is physically more plausible to consider the energy losses, since charged particles interact with the cosmic background of photons — producing pions, electron-positron pairs, and, in case of nuclei, undergoing photodesintegration processes —, and, for cosmologic distances of propagation, adiabatic losses due to cosmic expansion are considered. We approximated the energy losses by parameterizing, at each time step, the mean energy loss length,

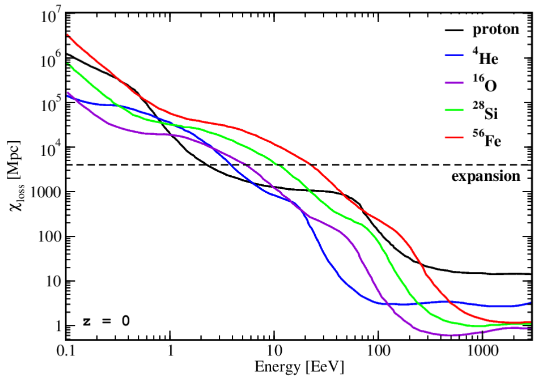

Figure 3: The total energy loss length, χ_{loss}, as a function of the energy for different nuclei (colors). The horizontal dashed line indicates the effect of the adiabatic expansion of the Universe. Adapted from [4].

χ_{loss}, as given in figure 3, which contains the contributions due to each one of these processes for different compositions of the UHECRs.

For cosmological distances of propagation, effects from the expansion of the universe must be taken into account. Due to the higher density cosmic baground of photons at a previous epoch, the density of photons at a distance corresponding to a redshift z is $n_\gamma \propto (1+z)^3$. As a consequence, the energy loss length at the redshift z can also be obtained from the value in the local universe by using this scaling law. **EGCRProp** takes the energy loss lengths χ_{loss}, as shown in figure 3, corrected by the particle redshift z.

5. Results

In the following, we present some results obtained from **EGCRProp**. First, we evaluated the code's energy conservation for the motions across our model of universe. The results are given in figure 4 for particles of 3.0 EeV and different compositions. As one can see, the relative deviations from initial particle energy $\delta E/E_0$ were very small, around $\sim 3,2\times 10^{-30}$ for protons and $\sim 2,0\times 10^{-33}$ for iron nuclei.

Second, we present the influence of the particle's magnetic rigidity on its propagation regime. The particle's magnetic rigidity, $R = E/Ze$, and the Larmor radius of the particle's trajectory, r_{L}, are corelated with the magnetic field strength, B, as follows:

$$\left(\frac{r_{\text{L}}}{\text{Mpc}}\right) = 1.1\left(\frac{R}{\text{EV}}\right)\left(\frac{\text{nG}}{B}\right). \tag{5.1}$$

For a given strength of the magnetic field, the higher the particle's magnetic rigidity, the bigger the Larmor radius of the particle's trajectory. In figure 5, we show the two-dimentional trajectory projections for two nuclei limiting the traveled distance up to 75.0 Mpc. We simulated the propagation of particles with six energies ranging from 3.0 EeV to 1000.0 EeV, without energy losses, for the two compositions. As expected the higher is the particle's energy, the less the particle's trajectory will be bent. In figure 6, we show the trajectories of different particle species for two given ener-

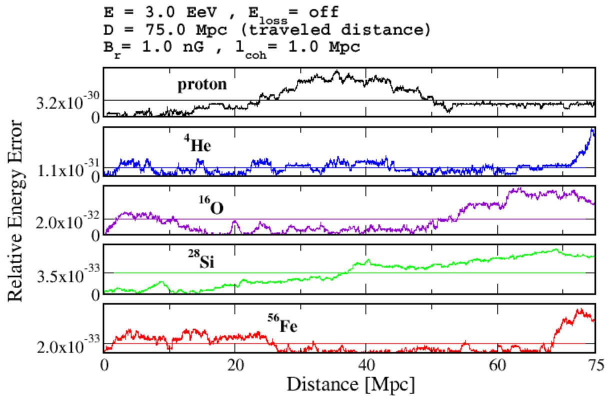

Figure 4: $\delta E/E_0$ as a function of the traveled distance for 5 different nuclei (colors) with $E_0 = 3.0$ EeV. The horizontal line indicates the average value after 75 Mpc.

gies. As expected the bigger is the particle's atomic number, the more the particle's trajectory will be bent.

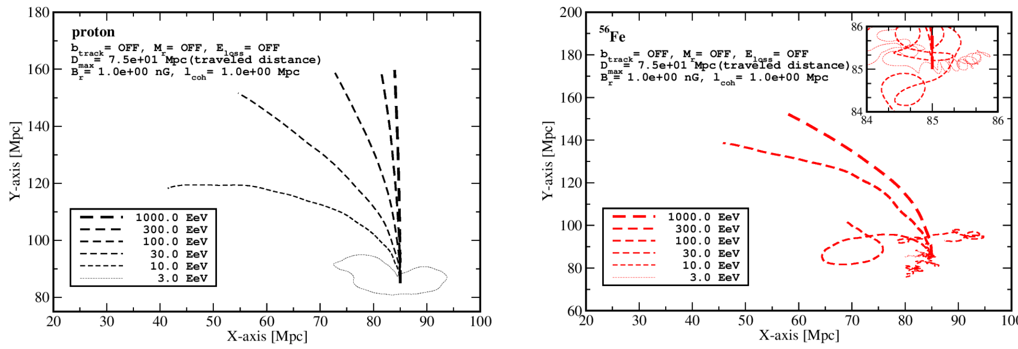

Figure 5: Two-dimensional projections for the trajectories in EGMFs for protons (left) and iron nuclei (right), with different given energies.

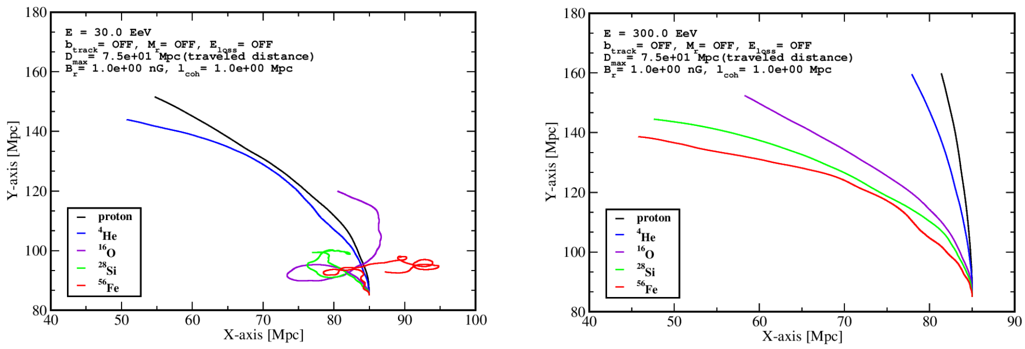

Figure 6: Two-dimensional projections for the trajectory in EGMFs for several nuclei (colors) of fixed energies: $E = 30.0\,$EeV (left) and $E = 300.0\,$EeV (right).

In third place, we studied the distance amplification from a rectilinear path after multiple scatterings. The results are given in figure 7 as functions of the distance traveled for three different magnetic rigidities (left) and of the energy for some interesting distances (right), corresponding to: Centaurus A (~ 3.8 Mpc), Virgo A (~ 17 Mpc), and two arbitrary distances of 50 Mpc, and 75 Mpc. In both plots, the lines show fits of parameterization functions, and the "x" symbols indicate the results from the simulation. In the left panel, the distances up to which the magnetic field effects are utterly negligible are indicated by vertical arrows, i.e. at: ~ 5 Mpc for $R = 3.0$ EV, ~ 8 Mpc for $R = 30.0$ EV, and ~ 8 Mpc for $R = 100.0$ EeV. These results clearly show when it is necessary to consider a full three-dimensional simulation, like **EGCRProp**.

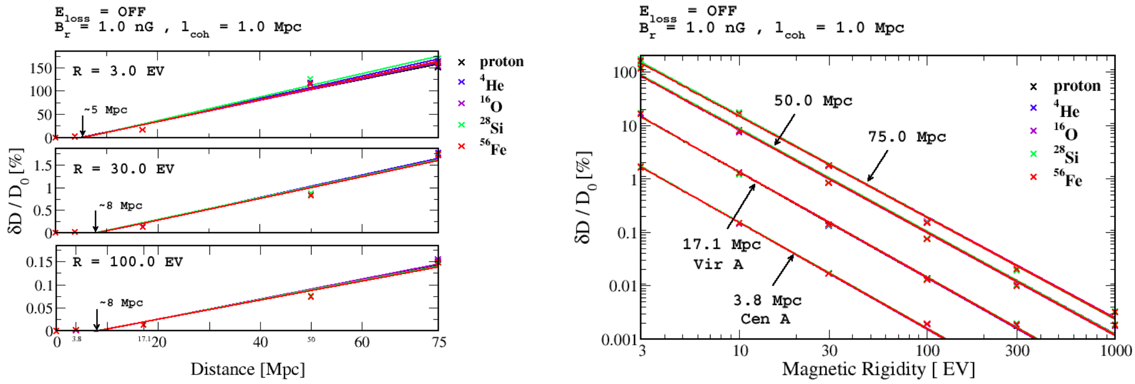

Figure 7: The distance amplifications, $\delta D/D_0[\%]$, for several nuclei (colors) with no energy losses, given as functions: of the traveled distance and three given magnetic rigidities (left); and of the rigidity for five different distances (right). See text for further details.

Finally, we compared the results from the simulations and the analytical predictions for the final scattering angle. In figure 8, the final scattering angle is plotted against the particle rigidity for different primaries and source distances. The analytical predictions are given by the dashed lines while the full lines give the fits obtained from the simulated points ("x" symbols). As one can see, the final scattering angles do not behave exactly as expected for small distances, while it is clear that for great distances there is an approximation of the simulations with the analytical predictions. In the limit $D/l_{\rm coh} \gg 1$, one can regard that the two curves will be approximately equal. Since the analytical functions for the final scattering angle are usually given by an expression like:

$$\theta \simeq 35^\circ \left(\frac{\rm EeV}{E/Z}\right)\left(\frac{B}{\rm nG}\right)\left(\frac{l_{\rm coh}}{\rm Mpc}\right)^{1/2}\left(\frac{D}{\rm Mpc}\right)^{1/2}, \tag{5.2}$$

and because the length traveled inside each cell is not fixed, we have defined an effective coherence length that actually dependends on the particle's energy:

$$\left(\frac{l_{\rm coh,eff}}{\rm Mpc}\right)^{1/2} = \alpha\left(\frac{E/Z}{\rm EeV}\right)^{0.1}\left(\frac{l_{\rm coh}}{\rm Mpc}\right)^{1/2}, \tag{5.3}$$

where α is a parameter to be determined.

Substituting $l_{\rm coh}$ in equation 5.2 by $l_{\rm coh,eff}$ and taking the values for α for each distance, we have found the parameterization for the final scattering angle with high accuracy. In figure 9, we

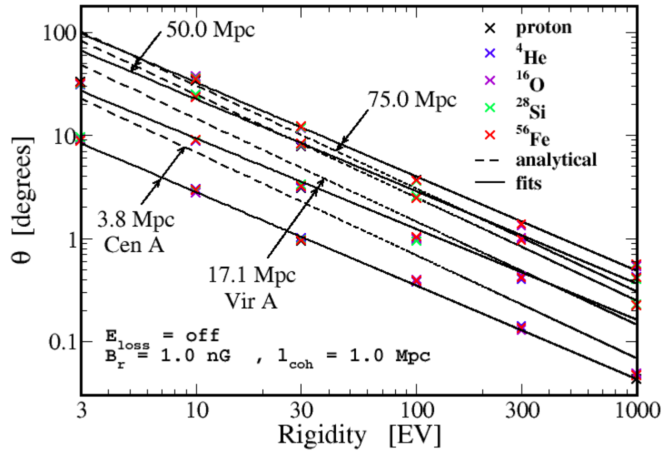

Figure 8: The dependence of the final scattering angle on the rigidity R for different primaries and distances to the sources. See text for further details.

show the results for this parameter as function of the distance. Taking a linear regression gives:

$$\alpha \approx 0.3 + 8 \times 10^{-3} D\,[\mathrm{Mpc}]. \tag{5.4}$$

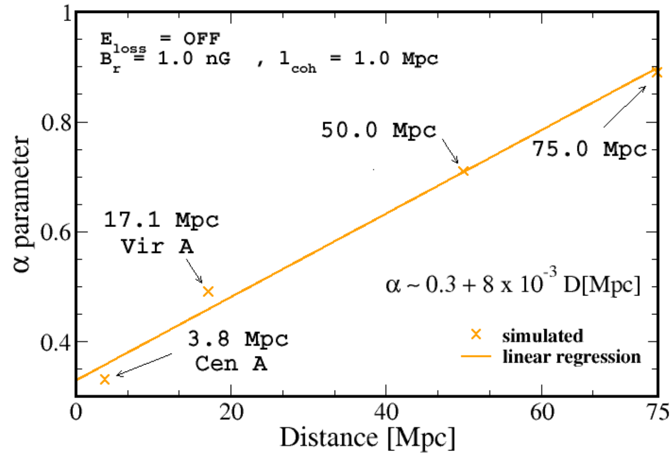

Figure 9: The parameter α as a function of the traveled distance. (See text for further details.)

6. Conclusions

EGCRProp is a novel fast Monte Carlo code for the propagation of UHECRs in the EGMFs medium. We presented in this paper its main features and some interesting results. The precision on the energy conservation within typical magnetic domains has been evaluated $\lesssim 3{,}2 \times 10^{-30}$. The influence of the particles' rigidities have been tested. The devations from a rectilinear path under different conditions, and the parameterizations for the scattering angle have been studied. Further results and studies can be found in the Ph.D. thesis in [5].

References

[1] M.A. Leigui de Oliveira, and R.P. Costa Junior. "A numerical model for the propagation of ultra-high energy cosmic rays through extragalactic magnetic fields", Proc. of the 35th ICRC (ICRC2017), PoS(ICRC2017)477.

[2] http://pesquisa.ufabc.edu.br/egcrprop/

[3] R.P. Costa Jr., and M.A. Leigui de Oliveira, "Analysis of the performance of numerical integration methods for the tracking of ultra-high energy cosmic rays", J. of Comp. Phys., **392**, (2019) 432-443, https://doi.org/10.1016/j.jcp.2019.04.058

[4] D. Allard, "Extragalactic propagation of ultra-high energy cosmic rays" *Astrop. Phys.*, **39-40** (2012) 33, arXiv:1111.3290v1 [astro-ph.HE] (2011).

[5] R.P. Costa Jr., "Propagation of ultra-high energy cosmic rays in extragalactic magnetic fields", Ph.D. thesis, UFABC (2019) Brazil.